

This is the peer reviewed version of the following article:

Antitumor Virotherapy Using Syngeneic or Allogeneic Mesenchymal Stem Cell Carriers Induces Systemic Immune Response and Intratumoral Leukocyte Infiltration in Mice

Álvaro Morales-Molina, Stefano Gambera, Teresa Cejalvo, Rafael Moreno, Miguel Ángel Rodríguez-Milla, Ana Judith Perisé-Barrios & Javier García-Castro

Cancer Immunol Immunother. 2018 Oct;67(10):1589-1602.

which has been published in final form at

<https://doi.org/10.1007/s00262-018-2220-2>

Antitumor virotherapy using syngeneic or allogeneic mesenchymal stem cell carriers induces systemic immune response and intratumoral leukocyte infiltration

Álvaro Morales-Molina¹, Stefano Gambera¹, Teresa Cejalvo¹, Rafael Moreno², Miguel Ángel Rodríguez-Milla¹, Ana Judith Perisé-Barrios¹, Javier García-Castro¹

¹ Cellular Biotechnology Unit, Institute of Health Carlos III, Madrid, E-28220, Spain.

² Virotherapy and Gene therapy Group, ProCure Program, Translational Research Laboratory, Instituto Catalan de Oncologia-IDIBELL, Barcelona, Spain.

Contact Information:

Javier García-Castro, PhD.
Instituto de Salud Carlos III
lab. 51-00-031
Ctra Majadahonda-Pozuelo, Km 2
E-28220 - Majadahonda (Madrid)
Spain

Phone: +34918223288
Fax: +34918223269
E-mail: jgcastro@isciii.es

Keywords: oncolytic virus; mesenchymal stem cells; carrier; tumor infiltration; immune response, Celyvir; immunotherapy

Abstract

Oncolytic virotherapy uses oncolytic viruses that selectively replicate in cancer cells. The use of cellular vehicles with migration ability to tumors has been considered to increase their delivery to target sites. Following this approach, the antitumor efficacy of the treatment Celyvir (mesenchymal stem cells infected with the oncolytic adenovirus ICOVIR-5) has been demonstrated in patients with neuroblastoma. However, the better efficacy of syngeneic or allogeneic mesenchymal stem cells as cell carriers and the specific role of the immune system in this therapy are still unknown.

In this study we use our virotherapy Celyvir with syngeneic and allogeneic mouse mesenchymal stem cells to determine their antitumor efficacy in a C57BL/6 murine adenocarcinoma model. Adoptive transfer of splenocytes from treated mice to new tumor-bearing mice followed by a secondary adoptive transfer to a third group was performed.

Similar reduction of tumor growth and systemic activation of the innate and adaptive immune system was observed in groups treated with syngeneic or allogeneic mesenchymal stem cells loaded with ICOVIR-5. Moreover, a different pattern of infiltration was observed by immunofluorescence in Celyvir-treated groups. While non-treated tumors presented higher density of infiltrating immune cells in the periphery of the tumor, both syngeneic and allogeneic Celyvir-treated groups presented higher infiltration of CD45+ cells in the core of the tumor. Therefore, these results suggest that syngeneic and allogeneic Celyvir induces systemic activation of the immune system, antitumoral effect and a higher intratumoral infiltration of leukocytes.

Précis

A similar reduction of tumor growth and systemic activation of immune system is observed using either syngeneic or allogeneic mesenchymal stem cells as carriers for an oncolytic adenovirus in the Celyvir treatment, both inducing a higher infiltration of leukocytes in the core of the tumor.

Abbreviations

Celyvir	Mesenchymal stem cells infected with ICOVIR-5
DMEM	Dulbecco's Modified Eagle's Media
hMSC	Human mesenchymal stem cells
IFN- γ	Interferon gamma
mMSC	Murine mesenchymal stem cells
mCelyvir	Murine mesenchymal stem cells infected with ICOVIR-5
MOI	Multiplicity of infection
MSC	Mesenchymal stem cells
pAkt	Phosphorylated Akt protein
TNF	Tumor Necrosis Factor

Introduction

Oncolytic virotherapy is an antitumor strategy based on the use of oncolytic viruses that selectively replicate in, and therefore lyse, tumor cells without causing damage in healthy cells. Its clinical interest does not only rely on the oncolytic response of the virus by its own, but also in the antitumor immune response that seems to be activated in treated patients [1].

To increase the life time of the oncolytic virus and the evasion of the antiviral immune response of the patient, a new approach based on the use of cell vehicles to transport the oncolytic virus has been considered. Moreover, the use of cells able to migrate to tumor microenvironments as cell carriers would also enhance the effectiveness of the treatment by increasing the number of viral particles that are released locally after its systemic administration.

Meeting these characteristics, mesenchymal stem cells (MSC) present high ability to migrate to solid tumors and inflamed areas [2, 3]. In addition to their employment for other indications, gene-modified MSC are being used in different clinical trials for the treatment of cancer (ClinicalTrials.gov identifier: NCT02079324) and in oncolytic virotherapies acting as carrier cells for an oncolytic measles virus (NCT02068794) and an oncolytic adenovirus (NCT01844661).

Following this approach, our research group has been working for more than 15 years in the use of Celyvir: MSC loaded with ICOVIR-5, a human oncolytic adenovirus [4]. This virus presents different modifications that restrict its replication to cells in which the retinoblastoma pathway is deregulated, a common characteristic in cancer cells [5]. The clinical use of Celyvir has already been demonstrated in a compassionate program with human patients and a clinical trial (NCT01844661) with children presenting refractory tumors –mainly neuroblastomas– in which complete remissions were achieved [6, 7]. The efficacy of the treatment has also been tested in murine models with human glioma xenografts [8, 9], semi-permissive cotton rat models [10] and immunocompetent murine models [11]. It has also been demonstrated that the administration of virus-loaded MSC induces a better antitumor effect than intratumoral administration of ICOVIR-5 alone [12]. This may suggest a more complex effect of the MSC by their own further than acting as simple cell carriers. However, further research is still needed to understand the complete mechanism of action of Celyvir.

Despite different studies have demonstrated the possibility of using allogeneic MSC to treat a variety of indications in contrast to a customized autologous cell therapy [13-15], there is still some controversy in their use as universal donor cells, as they have been considered immune evasive, but not immunoprivileged [16]. Moreover, there is even less evidence about the possible differential effect in using allogeneic or syngeneic MSC as carrier cells for oncolytic virotherapy.

Therefore, we here report the first comparison of syngeneic and allogeneic MSC as delivery vehicles for an oncolytic adenovirus by testing whether syngeneic or allogeneic murine MSC (mMSC) in Celyvir can be used as antitumoral treatment in a murine adenocarcinoma model. We find that both syngeneic and allogeneic mCelyvir resulting in the same pattern of systemic immune response and also present similar antitumor efficacy and intratumoral infiltration of leukocytes.

Materials and Methods

Cell culture

mMSC were obtained as previously described [17] from adipose tissue of C57BL/6J mice for syngeneic treatments, and from C57BL/10J mice for allogeneic treatments. mMSC characterization was verified by fibroblast morphology of adherent cells and protein expression profile analysis by flow cytometry. CMT64-6 clone was derived [12] from parental CMT 64 cell line, a murine non-small-cell lung carcinoma. Cells were cultured in complete Dulbecco's Modified Eagle's Media (DMEM) (Lonza): DMEM supplemented with 10% fetal bovine serum (FBS) (Sigma-Aldrich), streptomycin (100 mg/mL), penicillin (100 U/mL) and glutamine (2 mM) (Lonza); at 37 °C in a humidified atmosphere with 5% CO₂.

Viral infection with oncolytic adenovirus ICOVIR-5

1x10⁶ mMSC were infected with ICOVIR-5 at a multiplicity of infection (MOI) of 200 in 1 ml during 2 h at 37 °C in DMEM without FBS. Cells were washed 2 times with phosphate-buffered saline (PBS) to remove the virus from the cell culture supernatant. Infected mMSC are named mCelyvir.

NF-κB reporter luciferase assay

The activation of NF-κB was evaluated by using a luciferase reporter system [18]. mMSCs were transduced overnight with a non-replicative lentiviral vector that contains the pHAGE NF-κB-TA-LUC-UBC-GFP-W plasmid (Addgene plasmid #49343). Cells were infected with ICOVIR-5 and 1x10⁴ cells per well were seeded in 96-well plates with complete DMEM. After 24 h, cell lysis for total protein extraction was carried out and luciferase activity was assayed with the Luciferase Assay System (Promega Corporation).

Western Blot

5x10⁵ cells/well were seeded in 6-well plates with complete DMEM. After 3 and 24 h of treatment, total proteins were extracted with SDS sample buffer and protease inhibitor cocktail (Sigma-Aldrich). Proteins were separated by electrophoresis, transferred to PVDF membranes (Bio-Rad) and blocked with 2% milk in tris-buffered saline (TBS). Mouse monoclonal antibodies c-Jun (clone 3/Jun), phospho-Akt (Ser473, 2118;

Epitomics) and anti- β -actin (AC-15; Sigma-Aldrich) were used as primary antibodies. Polyclonal goat anti-rabbit and anti-mouse immunoglobulins/HRP (Dako) were used as secondary antibodies. Membranes were digitized and protein expression was quantified using Image J.

Cytokine array

Secreted cytokines were analyzed in mMSC and mCelyvir by cytokine array assay. 4×10^4 cells per well were seeded in 24-well plates with complete DMEM. After 24 h, supernatants were collected and pro-inflammatory cytokine pattern was analyzed using Proteome Profiler Mouse Array Panel A kit according to manufacturer's indications (R&D Systems, Minneapolis, MN). Secreted cytokine profile was measured semi-quantitatively by pixel density of duplicated spots. CXCL10 levels were quantified using Mouse CRG-2/IP-10 Ray Bio ELISA Kit (RayBiotech).

Direct and indirect co-culture of mMSC/mCelyvir and CMT64-6 cells

For direct co-culture, 1×10^5 CMT64-6 cells and 1×10^5 mMSC/mCelyvir per well were seeded in 6-well plates. 60 h later, supernatant and cells were obtained, blocked and labeled with anti-CD90 antibody (Miltenyi Biotec). For transwell co-culture, 5×10^4 CMT64-6 cells per well were seeded in 24-well plates and 5×10^4 mMSC/mCelyvir seeded in transwells (8 μ m pore filters, BD Biosciences) coated with 0.1% gelatin (Sigma-Aldrich) for 48 h. Apoptosis was quantified in CMT64-6 (CD90 negative) cells using Annexin V apoptosis detection kit (BD Pharmingen). CMT64-6 cells seeded alone were used as negative control, while CMT64-6 cells infected with ICOVIR-5 (MOI 200) were used as Annexin V positive control.

Migration assay

Cell migration towards tumor cells was studied *in vitro*. 24 well-plate transwells were coated with 0.1% gelatin and 5×10^4 cells were seeded in this upper chamber. 1×10^5 CMT64-6 cells/well were seeded in the bottom chamber as stimuli. Incubation of mMSC in the presence of DMEM alone was used as negative control. After 24 h, non-migrated cells were removed and migrated cells were fixed and stained with crystal violet. Cells from 13 high-power fields (HPF) (200X) were counted for each condition. For statistical analysis, the mean of migrated cells per HPF (cells/HPF) of each condition was compared (n=3).

Animal experiments

For *in vivo* homing of mCelyvir to the tumor, cells were labeled with 8.33 mg/ml DIR buffer for 30 min at 37 °C according to the protocol of XenoLight Dir (Caliper Lifesciences). Subcutaneous tumors were established in 7 week-old C57BL/6J mice by injecting 1×10^6 CMT64-6 cells transduced with a lentiviral vector containing a firefly luciferase cassette (referred to as CMT64-Luc). 1×10^6 DIR-labeled mCelyvir cells/mouse were intraperitoneally injected and fluorescent signal was measured 48 h later by IVIS 200 imaging system (Caliper). Non-stained mCelyvir were used as negative control. Bioluminescence images of the CMT64-Luc tumors were also obtained after intravenous injection of 150 mg/kg body weight of firefly luciferin (Promega). For *ex vivo* imaging, tumors were collected 48 h after mCelyvir administration and images were quantified using Living Image software (Xenogen). Peripheral blood samples were also collected at 48 h for flow cytometry analysis.

For *in vivo* antitumor efficacy experiments, subcutaneous tumors were established by injecting 1×10^6 CMT64-6 cells diluted in PBS into 7 week-old female C57BL/6J mice. According to the treatment, groups were assigned as PBS (n=12), syngeneic mMSC (n=5), allogeneic mMSC (n=5), syngeneic mCelyvir (n=5), or allogeneic mCelyvir (n=6). Treatment started at day 9 after tumor inoculation, with doses established as 5×10^5 cells/mouse resuspended in PBS intraperitoneally injected. A total of 4 doses were administered, separated by 5-7 days from one another. Tumor length (L), width (W) and height (H) were measured with a caliper every 3-5 days and tumor volume was calculated as $(L \times W \times H) \pi / 6$. Mice presenting tumor volumes smaller than the mean of the PBS group were considered as responders. The experiment was repeated 2 times. 28 days after tumor inoculation mice were sacrificed and tumors and spleens were processed for flow cytometry and histology analysis.

The study obtained an Animal Ethics Committee approval in compliance with European Union Directive 2010/63/UE. Animal care and experiments were carried out as per the guidelines detailed in Royal Decree 53/2013 of Spain.

Adoptive transfer of splenocytes

Spleens from previous treated mice of each group (PBS, syngeneic mCelyvir, and allogeneic mCelyvir) were mashed through a sterile 70 μ M nylon mesh cell strainer using

the rubber end of a syringe into PBS, and erythrocytes were lysed with Quicklysis buffer (Cytognos). Subcutaneous CMT64-6 tumors were established into 7-week-old female C57BL/6J mice as described above and randomly divided in three homogeneous groups (n=5). Three days after tumor inoculation, 3×10^7 splenocytes were transferred intravenously to each CMT64-6 tumor-bearing mouse. A secondary adoptive transfer of splenocytes from these mice to new CMT64-6 tumor-bearing C57BL/6J mice was performed following the same protocol. 28 days after each adoptive transfer of splenocytes, mice were sacrificed and tumors were processed for flow cytometry and histopathological analysis.

Flow cytometry

Extracted tumors were digested with collagenase IV (1 mg/ml) and mechanically homogenized using a potter-elvehjem PTFE pestle when necessary. Cell suspensions obtained from peripheral blood, digested tumors and spleens were filtered through a sterile 70 μ M nylon mesh cell strainer and red blood cells were lysed by incubation with Quicklysis buffer (Cytognos). Cell suspensions were blocked with mouse FcR Blocking (Miltenyi) for 15 min and incubated with the following mouse monoclonal antibodies for 20 min at 4 °C: CD45 (clone 30-F11), CD3 (145-2C11), CD4 (GK1.5), CD8 (53-6.7), CD11b (M1/70), CD11c (N418), CD206 (C068C2), MHCII (M5/114.15.2), Ly6C (AL-21), Ly6G (1A8-Ly6g), and NK1.1 (PK136) (eBioScience). After incubation, cells were labeled with the viability marker 7AAD (Fisher Scientific). Samples were acquired with MACSQuant Analyzer cytometer and analyzed using MACSQuantify analysis software (Miltenyi Biotec).

Tumor histology and immunohistochemistry

Tumor samples were fixed and embedded within Optimal Cutting Temperature medium (Tissue-Tek). 8 μ m thick sections were obtained and stained with hematoxylin and eosin. For immunohistochemistry analysis, samples were incubated with Avidin/Biotin blocking kit (Vector Laboratories, Burlingame, CA) and incubated with primary biotin rat anti-mouse CD45 antibody (clone 30-F11, 10 mg/ml) (eBioscience) followed by incubation with Alexa Fluor 546 streptavidin conjugate/secondary antibody (Invitrogen). Meter ANTICUERPO ADENO Nuclei were counterstained with DAPI (5 μ g/ml). Signal was detected with a Leica TCS SP5 multispectral microscope (Leica Microsystems). Representative maps were obtained by maximum projection of 5 stacks and analyzed

using Leica LAS AF (Wetzlar). For quantification of CD45 antibody expression in the core and periphery of the tumors, a region of interest (ROI) of $600 \mu\text{m}^2$ was employed to measure the mean fluorescence intensity (MFI) in different stacks (n=6).

Statistical analysis

Data was analyzed and graphed with GraphPad Prism (GraphPad Software). *In vitro* results were expressed as the mean \pm SD and *in vivo* results were expressed as the mean \pm SEM. Significant differences were determined using paired or non-paired non-parametric test (Mann-Whitney *U* test or Will-Coxon test, respectively). $P < 0.05$ (*), $P < 0.01$ (**) and $P < 0.001$ (***) were deemed statistically significant.

Results

C57BL/6 and C57BL/10 mMSC present similar molecular signaling activation after infection with ICOVIR-5

To analyze activation in response to adenoviral infection, mMSC were transduced with a lentiviral vector that contains a promoter for response by luminescence to activation of the NF- κ B pathway, so activation of the pathway is translated into luciferase expression [18]. However, luciferase activity did not increase after adenoviral infection in C57BL/6 or C57BL/10 cells, and no significant differences in NF- κ B pathway activation were observed between both cell types (Fig. 1a).

We previously studied other signaling pathways in mMSC after adenoviral infection [12], so we analyzed Jun and phospho-Akt (pAkt) in mMSC and mCelyvir at 3 and 24 h by Western Blot (Fig. 1d). At basal non-infected state, expression of Jun and pAkt was significantly lower in C57BL/6 mMSC than in C57BL/10 mMSC at 24 h. However, no significant differences in Jun or pAkt levels were observed between C57BL/6 and C57BL/10 mCelyvir at 24 h (Fig. 1 b and c). This is due to the increased expression of Jun and pAkt in C57BL/6 cells after infection with ICOVIR-5, not seen in C57BL/10 cells. Consequently, significant higher mCelyvir/mMSC Jun and pAkt expression ratios were observed in C57BL/6 cells than in C57BL/10 cells (Fig. 1e and f). This data suggest that C57BL/6 and C57BL/10 cells present the same response after loading with the oncolytic virus in spite of their different basal signaling.

C57BL/6 and C57BL/10 mMSC present a similar cytokine secretion profile after infection with ICOVIR-5

We also studied the secretome response to ICOVIR-5 infection by performing a secretion array panel of 40 pro-inflammatory cytokines. At a basal state, both C57BL/6 and C57BL/10 mMSC secreted some cytokines, such as IL-6, which is highly expressed by pro-inflammatory mMSC (Fig. 1g). However, semi-quantification of secreted cytokines in C57BL/10 mMSC showed a higher basal secretion of CD54, CXCL10, CCL5 and CXCL12 than in C57BL/6 mMSC (Fig. 1h). Nevertheless, no relevant differences were observed between C57BL/6 and C57BL/10 mCelyvir apart from CXCL10. Indeed, CXCL10 was the only pro-inflammatory cytokine that remarkably increased after infection with ICOVIR-5 in C57BL/6 cells. Quantification of CXCL10 secretion by

ELISA assay confirmed this significant increase in C57BL/6 cells after adenoviral infection, while both C57BL/10 mMSC and mCelyvir secreted similar moderate levels of CXCL10 (Fig. 1i).

In summary, these results indicate that C57BL/10 mMSC present a higher basal secretion of pro-inflammatory cytokines than C57BL/6 mMSC. However, with the exception of CXCL10, no differences were observed between C57BL/6 and C57BL/10 mCelyvir.

C57BL/6 and C57BL/10 mMSC do not induce *in vitro* antitumor effect.

To study the effect of the MSC on CTM64-6 cells, at basal state and after infection with ICOVIR-5, direct and transwell co-culture of mMSC or mCelyvir with CMT64-6 cells were performed. As we wanted to study the antitumoral effect of the mMSC by itself (and not by the oncolytic virus), the experiment was carried out 72 h after adenoviral to avoid the effect of a potential release of virus from the mMSC. As seen in Fig. 1j, neither C57BL/6 nor C57BL/10 mMSC or mCelyvir cells induced an apoptotic effect on CMT64-6 cells by their own, resulting in similar death percentage as the negative control (CMT64-6 cells alone) (Fig.1l). Similarly, no apoptotic effect on tumor cells was observed after exposition to secreted factors from any cells or condition (Fig. 1k). These results indicate that C57BL/6 and C57BL/10 mMSC do not induce an antitumor effect by themselves *in vitro*, neither by direct contact nor through some factor secretion, as it does the oncolytic virus ICOVIR-5 alone (Fig. 1l).

***In vitro* and *in vivo* tumoral homing of syngeneic and allogeneic mCelyvir**

Tumoral homing ability of mMSC and mCelyvir towards CMT64-6 cells was studied *in vitro* and *in vivo*. *In vitro* transwell migration assay demonstrated that both mock- and infected- C57BL/6 and C57BL/10 cells present significant intrinsic migration ability at 24 h compared to the negative control, in which barely any cell migrated (Fig. 2a). Quantification of migrated cells showed a slightly higher migration of C57BL/6 mMSC and mCelyvir toward the CMT64-6 cells stimuli compared with that of C57BL/10 cells, but no significance was observed (Fig. 2b). Moreover, similar mCelyvir/mMSC migration ratio was observed in both C57BL/6 and C57BL/10 cells (Fig. 3c). These results indicate the mMSC carrying the oncolytic virus ICOVIR-5 maintains the intrinsic migration ability of mMSC toward CMT64-6 tumor cells.

As a suitable cell carrier must successfully home into the tumor, tracking of syngeneic C57BL/6 and allogeneic C57BL/10 mCelyvir treatments were also studied *in vivo* in mice bearing CMT64-Luc tumors. 48 h after intraperitoneal administration of the treatment, a localized homing of both C57BL/6 and C57BL/10 mCelyvir was detectable in colocalization with the CMT64-Luc tumor site (Fig. 2d). *Ex vivo* tumor quantification showed no significant differences in homing of syngeneic and allogeneic mCelyvir treatment at 48 h (Fig. 2e).

Peripheral blood immune activation after allogeneic and syngeneic mCelyvir administration

The innate response of immune system against the virus-infected mMSC may be crucial for the proper antitumor effect, especially after administration of allogeneic mCelyvir. Therefore, we studied the general immune stimulation in peripheral blood at 48 h after administration of the treatment, in immunocompetent CMT64-6-tumor bearing mice. A significant increase in neutrophils and monocytes were observed in groups treated with syngeneic and allogeneic mCelyvir compared to the non-treated group (Fig. 3b). A significant increase of Natural Killer (NK) cells was also observed after administration of allogeneic mCelyvir, which was not observed in group treated with syngeneic mCelyvir (Fig. 3b). We also studied the adaptive immune response to the treatment, but no differences in total leukocytes, T cells or CD4/CD8 ratio were observed between mCelyvir-treated and non-treated mice (Fig. 3b).

Allogeneic and syngeneic mCelyvir-treated groups present similar tumor growth

To determine the *in vivo* biological effect, we compared the antitumor efficacy of syngeneic or allogeneic mCelyvir in C57BL/6J mice bearing CMT64-6 tumors, as well as the effect of syngeneic or allogeneic mMSC as an additional control (Fig. 3a). Both syngeneic and allogeneic mCelyvir groups presented a similar antitumor tendency compared to the PBS group (35%), but no statistical significance was obtained (Fig. 3c). As showed in Fig. 3d, 60% of the mice treated with syngeneic mCelyvir and 66% of the mice treated with allogeneic mCelyvir responded to the treatment, presenting smaller tumor volumes than the mean of the PBS group at the end point (30 days). Administration of syngeneic or allogeneic mMSC (without the oncolytic virus) did not induce an antitumor effect, resulting in similar outcomes as the PBS group (Fig. 3d and

Supplementary Fig. 1). These data suggest that both syngeneic and allogeneic mCelyvir induce similar tendency to inhibit tumor growth, which is not caused by the mMSC alone.

mCelyvir treatment induces systemic changes in the composition of the immune system

To study the general activation of the immune system after long treatment with mCelyvir, spleens from treated mice were harvested and splenocytes were analyzed by flow cytometry. Interestingly, differences in innate and adaptive immune system were found between treated and non-treated mice. After mCelyvir administration, NK cells percentage was doubled, while proportion of myeloid cells notably decreased from 89.10% to 25% (Fig. 3e). An increase in total T cells from 7.85% to 30% was also observed, as well as changes in T cell subpopulations: cytotoxic CD8⁺ lymphocytes increased from 21.83% to 58% in both groups treated with syngeneic or allogeneic mCelyvir, while helper CD4⁺ lymphocytes decreased from 60.15% to 34%. These results indicate that mCelyvir treatment induces significant systemic changes in the composition of the immune system.

mCelyvir treatment increases N1/N2 neutrophils ratio in intratumoral immune subpopulations

To evaluate the intratumoral immune response to syngeneic or allogeneic mCelyvir treatment, tumors were harvested and infiltrating immune cells were analyzed by flow cytometry. As seen in Fig. 4a, no statistical differences in infiltration were observed in total leukocytes (CD45⁺), CD4⁺ or CD8⁺ T cells, NK cells, dendritic cells (NK1.1-CD11b⁺ CD11c⁺), or M1 (CD206⁻) and M2 (CD206⁺) macrophages (CD45⁺ CD11b-Ly6G⁻ MHCII⁺). However, a significant increase in N1/N2 ratio of neutrophils was observed in both syngeneic and allogeneic mCelyvir groups compared to the PBS group (Fig. 4a). This increase in the ratio is supported by a significant decrease in N2 subpopulation (CD206⁻) of neutrophils in the allogeneic mCelyvir group—similar to the observed in the syngeneic mCelyvir group—compared to the PBS group (Supplementary Fig. 2). In accordance with these results, we observed that lower volumes in mCelyvir-treated tumors significantly correlated with higher N1/N2 ratios and decreased levels of N2 neutrophils (Fig. 4b and c).

mCelyvir treatment increases infiltration of immune cells in the core of the tumor

To study the localization of tumor infiltrating immune cells, immunohistochemistry assay of CD45+ cells was performed. Interestingly, a different pattern of distribution of CD45+ cells was observed between PBS and mCelyvir-treated groups. These immune cells localized mainly to the periphery of PBS-treated tumors (Fig. 4d), which was not observed in syngeneic or allogeneic mCelyvir-treated tumors (Fig. 4e and f). Quantification of the CD45+ MFI confirmed a significant higher CD45+ expression in the periphery of PBS-treated tumors compared to the mCelyvir-treated groups. In contrast, a significant higher localization of CD45+ cells was observed in the core of allogeneic mCelyvir-treated tumors compared to the PBS-treated tumors (Fig. 4g). As a result, core/periphery expression ratio of CD45+ cells was similarly increased in both syngeneic and allogeneic mCelyvir-treated groups (Fig. 4h). These findings suggest that mCelyvir treatment induces an increased infiltration of leukocytes in the core of the tumor.

¿PRESENCIA DE VIRUS? ¿FOTOS? ¿CITAR AQUÍ?

Adoptive transfer of splenocytes preserves the antitumor efficacy

As we previously observed that mCelyvir treatment induced changes in the systemic immune system, we performed two consecutive adoptive transfers of splenocytes to study their activation. Splenocytes from previous treated mice were then harvested and transferred into new CMT64-6 tumor-bearing mice. Four weeks later, spleens from these transferred mice were obtained and splenocytes were transferred into a third group of CMT64-6 tumor bearing mice (Fig. 5a). In both groups transferred with splenocytes harvested from syngeneic or allogeneic mCelyvir-treated mice, 80% (4/5) of the mice responded to the treatment (Fig. 5b). This tendency to inhibit tumor growth was also preserved after the secondary adoptive transfer of splenocytes from these mice to new CMT64-6 tumor-bearing mice, in which 80% (4/5) of the mice were responders to the treatment (Fig. 5c). However, no statistical differences in tumor infiltrating immune cells were observed in any group after the first or secondary adoptive transfer of splenocytes (Fig. 5d and 5e).

Discussion

The use of MSC as cell vehicles for oncolytic viruses constitutes a novel and promising strategy to increase the effectiveness of oncolytic virotherapy. The antitumor effect of Celyvir treatment has been applied in children with refractory neuroblastomas, obtaining relevant clinical responses and even complete remissions [6, 7], with the remarkable absence of side effects [19]. The strategy has been also tested in canine patients with spontaneous tumors [Cejalvo *et al.*, unpublished results] and immunocompetent murine models [11, 12]. In general, murine cells do not support replication of human adenovirus [20, 21], then we previously generated the CMT64-6 cell line, a semi-permissive lung adenocarcinoma murine cell line that supports the complete replication cycle of human adenovirus [12, 22, 23]. Here, in this study, we demonstrated that the use of syngeneic or allogeneic mMSC as cell carriers for an oncolytic adenovirus induce similar systemic immune activation, antitumor tendency and infiltration of leukocytes in the core of the tumor

NF- κ B is an inducible transcription factor involved in many biological processes such as development, innate immunity and inflammation. Thus, increased activation of NF- κ B has been observed in human MSC in response to stress, cytokines, free radicals, hypoxia, and bacterial or viral antigens [24]. Surprisingly, no significant activation of NF- κ B was observed in C57BL/6 or C57BL/10 cells after ICOVIR-5 infection, in contrast to other studies indicating that NF- κ B is involved in adenoviral infection [25]. Moreover, products encoded by the E1a and E3 early genes of adenoviral serotype 5 have been associated with NF- κ B activation [26, 27]. However, it has also been reported that E1A protein can inhibit the activation of NF- κ B induced by tumor necrosis factor (TNF) through I κ Ba phosphorylation and suppression of IKK activity [28]. Similarly, proteins of viruses like hepatitis C virus can suppress NF- κ B activation through inhibition of I κ Ba degradation [29].

Typically, adenoviral infection induces the expression of pro-inflammatory cytokines such as IL-6, IL-8, TNF- α , CCL3 (also known as MIP-1a), CCL5 (also known as RANTES) and interferon-gamma (IFN- γ) in human cells [30]. Considering that we used a human adenovirus infecting murine MSC, a slightly different expression pattern could be expected. In our experiments, we observed an overexpression of IL-6, CXCL2, CXCL10, CCL2, CCL4 (also known as MIP-1b) or CCL5, but no remarkable expression

of CCL3, IFN- γ or TNF- α . The absence of secretion of these pro-inflammatory cytokines may be related to the non-activation of NF- κ B, as this transcription factor is required for transcription of TNF- α and other cytokines [31]. In this regard, expression of CXCL10 and other cytokines does not only promote MSC migration [32, 33], but also acts as a chemoattractant for activated T cells, monocytes and NK cells to the area of inflammation [34, 35]. Moreover, an activation of the innate response in peripheral blood is observed 48 hours after inoculation of the infected-mMSC, with increased proportions of neutrophils, monocytes and NK cells, which participates in the early control against virus-infected cells and general virus infection. Thus, the pro-inflammatory profile of cytokines after adenoviral infection of mMSC may be crucial after administration of mCelyvir.

The study of the immune system from the spleens after 30 days of treatment showed an activation of the adaptive immune response with increased proportions of T cells and CD8⁺ subpopulation, and a downregulation of the innate response with the exception of the NK subset. Initiation of the anti-tumor immune response may be then lead by the initial activation of the NK cells, whose cell-mediated killing of virus-infected cells also impacts in T cell responses (REFERENCIA Innate or adaptive immunity?). Moreover, it has been proposed that target-cell debris produced by NK cells may promote antigen cross-presentation to CD8⁺ T cells (REFERENCIA NK cell mediated killing of target cells triggers). As a result, the systemic activation of the immune system, together with the released viral particles and a local secretion of cytokines by the MSC in the tumor microenvironment, may break the immunologic tolerance and therefore enhance the activation of the antitumor immune response. However, in our murine model this activation seems to be braked because the antitumoral efficacy is limited.

Neutrophils show a polarization status, similar to macrophages: pro-inflammatory/anti-tumorigenic (N1) and anti-inflammatory/pro-tumorigenic (N2) phenotype [37]. In our model, flow cytometry analysis of tumor infiltration showed a significant increase in N1/N2 ratio in both syngeneic and allogeneic mCelyvir groups compared to the control group. Moreover, lower tumor volumes significantly correlated with higher N1/N2 ratios and lower N2 infiltration. As N2 phenotype contributes to tumor growth and immunosuppression, decrease of these neutrophils may be related to the observed tendency to inhibit tumor growth in our mCelyvir-treated groups. This correlation is consistent with previous studies in which depletion of pro-tumorigenic N2 neutrophils inhibited tumor growth and reduced immunosuppression in the tumor microenvironment,

even in the absence of CD8+ cells [38, 39]. Comparing mCelyvir- and PBS-treated groups, a different pattern of CD45+ infiltration was observed by immunohistochemistry study, in which treated tumors presented a significant higher infiltration of CD45+ cells in the core of the tumor. This higher core infiltration has been extensively associated with better prognosis in malignancies such as colorectal, ovarian, esophageal, and breast cancer [40-43]. In this regard, it has been shown that higher infiltration of leukocytes increases the therapeutic efficacy of immunotherapies in liver cancer and melanoma [44, 45]. Thus, Celyvir treatment may be considered in combination with other immunotherapies.

In conclusion, syngeneic or allogeneic mMSC could be used as cell carriers for the systemic delivery of oncolytic adenoviruses, both inducing a similar systemic immune response, antitumor efficacy and intratumoral infiltration of leukocytes. These results open the possibility of also using allogeneic MSC for the development of cell carrier-based virotherapies.

Compliance with Ethical Standards

Conflict of interest. The authors declare that they have no conflict of interest.

Acknowledgements. This work was supported by PI14CIII/00005 and PI17CIII/00013 grants to J G-C from the Ministerio de Economía y Competitividad of Spain and Asociación Pablo Ugarte (CIF G86121019). The authors would like to thank Isabel Cubillo, Alicia Giménez and Elena Calvo for their technical support in the study.

NK cell-mediated killing of target cells triggers robust antigen-specific T cell-mediated and humoral responses

[Philippe Krebs](#),¹ [Michael J. Barnes](#),¹ [Kristin Lampe](#),² [Karen Whitley](#),¹ [Keith S. Bahjat](#),³ [Bruce Beutler](#),¹ [Edith Janssen](#),² and [Kasper Hoebe](#)²

Innate or Adaptive Immunity? The Example of Natural Killer Cells

Eric Vivier,^{1,2,3,4,*†} David H. Raulet,^{5,†} Alessandro Moretta,^{6,†} Michael A. Caligiuri,^{7,†} Laurence Zitvogel,^{8,†} Lewis L. Lanier,^{9,†} Wayne M. Yokoyama,^{10,†} and Sophie Ugolini^{1,2,3,*†}

References

1. Russell SJ, Peng KW, Bell JC (2012) Oncolytic virotherapy. *Nat Biotechnol* 30(7):658-670.
2. Murphy MB, Moncivais K, Caplan AI (2013) Mesenchymal stem cells: environmentally responsible therapeutics for regenerative medicine. *Exp Mol Med* 45:e54.
3. Ramírez M, García-Castro J, Melen GJ, González-Murillo A, Franco-Luzón L (2015) Patient-derived mesenchymal stem cells as delivery vehicles for oncolytic virotherapy: novel state-of-the art technology. *Oncolytic Virotherapy* 4:149-155.
4. Alonso MM, Cascallo M, Gomez-Manzano C, Jiang H, Bekele BN, Perez-Gimenez A, Lang FF, Piao Y, Alemany R, Fueyo J (2007) ICOVIR-5 shows E2F1 addiction and potent antiglioma effect in vivo. *Cancer Res* 67(17):8255-8263.
5. Cascallo M, Alonso MM, Rojas JJ, Perez-Gimenez A, Fueyo J, Alemany R (2007) Systemic toxicity-efficacy profile of ICOVIR-5, a potent and selective oncolytic adenovirus based on the pRB pathway. *Mol Ther* 15(9):1607-1616.
6. García-Castro J, Alemany R, Cascalló M, Martinez-Quintanilla J, Arriero MdelM, Lassaletta A, Madero L, Ramirez M (2010) Treatment of metastatic neuroblastoma with systemic oncolytic virotherapy delivered by autologous mesenchymal stem cells: an exploratory study. *Cancer Gene Ther* 17(7):1667-1676.
7. Melen GJ, Franco-Luzon L, Ruano D, Gonzalez-Murillo A, Alfranca A, Casco F, Lassaletta A, Alonso M, Madero L, Alemany R, García-Castro J, Ramirez M (2016) Influence of carrier cells on the clinical outcome of children with neuroblastoma treated with high dose of oncolytic adenovirus delivered in mesenchymal stem cells. *Cancer Lett* 371:161-170.
8. Sonabend AM, Ulasov IV, Tyler MA, Rivera AA, Mathis JM, Lesniak MS (2008) Mesenchymal stem cells effectively deliver an oncolytic adenovirus to intracranial glioma. *Stem Cells* 26:831-841.
9. Martinez-Quintanilla J, He D, Wakimoto H, Alemany R, Shah K (2015) Encapsulated stem cells loaded with hyaluronidase-expressing oncolytic virus for brain tumor therapy. *Mol Ther* 23:831-841.

10. Ahmed AU, Rolle CE, Tyler MA, Han Y, Sengupta S, Wainwright DA, Balyasnikova IV, Ulasov IV, Lesniak MS (2010) Bone marrow mesenchymal stem cells loaded with an oncolytic adenovirus suppress the anti-adenoviral immune response in the cotton rat model. *Mol Ther* 18(10):1846-1856.
11. Rincon E, Kanojia D, Auffinger B, Ullyia I, Han Y, Alemany R, Ramirez M, García-Castro J, Lesniak M (2013) Therapeutic effect of mesenchymal stem cells in combination with oncolytic adenoviruses for the treatment of solid tumors in an immunocompetent mouse model (P2020). *J Immunol* 190:214.11.
12. Rincón E, Cejalvo T, Kanojia D, Alfranca A, Rodríguez-Milla MA, Hoyos RAG, Han Y, Zhang L, Alemany R, Lesniak MS, García-Castro J (2017) Mesenchymal stem cell carriers enhance antitumor efficacy of oncolytic adenoviruses in an immunocompetent mouse model. *Oncotarget* doi: 10.18632/oncotarget.17557
13. Zhang J, Huang X, Wang H, Liu X, Zhang T, Wang Y, Hu D (2015) The challenges and promises of allogeneic mesenchymal stem cells for use as a cell-based therapy. *Stem Cell Ther* 6:234.
14. Xu J, Wang D, Liu D, Fan Z, Zhang H, Liu O, Ding G, Gao R, Zhang C, Ding Y, Bromerg Ys, Chen W, Sun L, Wang S (2012) Allogeneic mesenchymal stem cell treatment alleviates experimental and clinical Sjögren syndrome. *Blood* 120(15):3142-3151.
15. Kavanagh H, Mahon BP (2011) Allogeneic mesenchymal stem cells prevent allergic airway inflammation by inducing murine regulatory T cells. *Allergy* 66(4):523-531.
16. Ankrum JA, Ong JF, Karp JM (2014) Mesenchymal stem cells: immune evasive, not immune privileged. *Nat Biotechnol* 32:252-260.
17. Mosna F, Sensebe L, Krampera M (2010) Human bone marrow and adipose tissue mesenchymal stem cells: a user's guide. *Stem Cells Dev* 19:1449-1470.
18. Wilson AA, Kwok LW, Porterl EL, Payne JG, McElroy GS, Ohle SJ, Greenhill SR, Blahna MT, Yamamoto J, Jean JC, Mizferd JP, Kotton DN (2013) Lentiviral delivery of RNAi for *in vivo* lineage-specific modulation of gene expression in mouse lung macrophages. *Mol Ther* 21:825-833.

19. Henaff D, Salinas S, Kremer E (2011) An adenovirus traffic update: from receptor engagement to the nuclear pore. *Future Microbiol* 6:179-192.
20. Duncan SJ, Gordon FC, Gregory DW, McPhie JL, Postlethwaite R, White R, Willcox HN (1978) Infection of mouse liver by human adenovirus type 5. *J Gen Virol* 40:45-61.
21. Starzinski-Powitz A, Schulz M, Esche H, Mukai N, Doerfler W (1982) The adenovirus type 12 – mouse cell system: permissivity and analysis of integration patterns of viral DNA in tumor cells. *EMBO J* 1:493-497.
22. Woller N, Knocke S, Mundt B, Gurlevik E, Struver N, Kloos A, Boozari B, Schache P, Manns MP, Malek NP, Sparwasser T, Zender L, Wirth TC, Kubicka S, Kühnel F (2011) Virus-induced tumor inflammation facilitates effective DC cancer immunotherapy in a Treg-dependent manner in mice. *J Clin Invest* 121(7):2570-2582.
23. Hallden G, Hill R, Wang Y, Anand A, Liu TC, Lemoine NR, Francis J, Hawkins L, Kirn D. Novel (2003) Novel immunocompetent murine tumor models for the assessment of replication-competent oncolytic adenovirus efficacy. *Mol Ther* 8:412-424.
24. Crisostomo PR, Wang Y, Markel TA, Wanq M, Lahm T, Meldrum DR (2008) Human mesenchymal stem cells stimulated by TNF- α , LPS, or hypoxia produce growth factors by an NF kappa B-but not JNK-dependent mechanism. *Am J Physiol Cell Physiol* 294(3):C675-682.
25. Melotti P, Nicolis E, Tamanini A, Rolfini R, Pavirani A, Cabrini G (2001) Activation of NF- κ B mediates ICAM-1 induction in respiratory cells exposed to an adenovirus-derived vector. *Gene Ther* 8(18):1436-1442.
26. Shurman L, Sen R, Bergman Y (1989) Adenovirus E1A products activate the Ig k-chain enhancer in fibroblasts. A possible involvement of the NF- κ B binding site. *J Immunol* 143(11):3806-3812.
27. Pahl HL, Sester M, Burgert HG, Baeuerle PA (1996) Activation of transcription factor NF-kappaB by the adenovirus E3/19K protein requires its ER retention. *J Cell Biol* 132(4):511-522.

28. Shao R, Hu MCT, Zhou BP, Lin S, Chiao PJ, von Lindern RH, Spohn B, Hung M (1999) E1A sensitizes cells to Tumor Necrosis Factor-induced apoptosis through inhibition of I κ B Kinases and Nuclear Factor κ B activities. *J Biol Chem* 274(31):21495-8.
29. Hiscott J, Kwon H, Génin P (2001) Hostile takeovers: viral appropriation of the NF-kappaB pathway. *J Clin Invest* 107(2):143-151.
30. Hendrickx R, Stichling N, Koelen J, Kuryk L, Lipiec A, Greber UF (2014) Innate immunity to adenovirus. *Hum Gene Ther* 25:265-284.
31. Mogensen TH, Paludan SR (2001) Molecular pathways in virus-induced cytokine production. *Microbiol Mol Biol Rev* 65(1):131-150.
32. Bernardo Me, Fibbe WE (2013) Mesenchymal stromal cells: sensors and switchers of inflammation. *Cell Stem Cell* 13:392-402.
33. Anton K, Banerjee D, Glod J (2012) Macrophage-associated mesenchymal stem cells assume an activated, migratory, pro-inflammatory phenotype with increased IL-6 and CXCL10 secretion. *PLoS One* 7(4):e35036.
34. Bonecchi R, Bianchi G, Bordignon PP ET AL. Differential expression of chemokine receptors and chemotactic responsiveness of type 1 T helper cells (Th1s) and Th2s (1998) *J Exp Med* 187:129-134.
35. Liu M, Guo S, Stiles JK (2011) The emerging role of CXCL10 in cancer. *Oncol Lett* 2(4):583-589.
36. Nishio N, Diaconu I, Liu H, Cerullo V, Caruana I, Hoyos V, Bouchier-Hayes L, Savoldo B, Dotti G (2014) Armed oncolytic virus enhances immune functions of chimeric antigen receptor-modified T cells in solid tumors. *Cancer Res* 74(18):5195-5205. QUITAR Y MOVER REFERENCIAS
37. Fridlender ZG, Sun J, Kim S, Kapoor V, Cheng G, Ling L, Worthen GS, Albelda SM (2009) Polarization of tumor-associated neutrophil phenotype by TGF-beta: "N1" versus "N2" TAN.
38. Pekarek LA, Starr BA, Toledano AY, Schreiber H (1995) Inhibition of tumor growth by elimination of granulocytes. *J Exp Med* 181:435-440.

39. Nozawa H, Chiu C, Hanahan D (2006) Infiltrating neutrophils mediate the initial angiogenic switch in a mouse model of multistage carcinogenesis. *Proc Natl Acad Sci USA* 103:12493-12498.
40. Dahlin AM, Henriksson ML, Van Guelpen B, Stenling R, Oberg A, Rutegard J, Palmqvist R (2011) Colorectal cancer prognosis depends on T-cell infiltration and molecular characteristics of the tumor. *Mod Pathol* 24(5):671-682.
41. Sato E, Olson SH, Ahn J, Bundy B, Nishikawa H, Qian F, Jungbluth AA, Frosina D, Gnjjatic S, Ambrosone C, Kepner J, Odunsi T, Ritter G, Lele S, Chen YT, Ohtani H, Old LJ, Odunsi K (2005) Intraepithelial CD8+ tumor-infiltrating lymphocytes and a high CD8+/regulatory T cell ratio are associated with favorable prognosis in ovarian cancer. *Proc Natl Acad Sci U S A* 102:18538-18543.
42. Schumacher K, Haensch W, Roefzaad C, Schlag PM (2001) Prognostic significance of activated CD8(+) T cell infiltrations within esophageal carcinomas. *Cancer Res* 61:3932-3936.
43. Dushyanthen S, Beavis Pa, Savas P, Teo ZL, Zhou C, Mansour M, Darcy PK, Loi S (2015) Relevance of tumor-infiltrating lymphocytes in breast cancer. *BMC Med* 13:202.
44. Wang HT, Lee HI, Guo JH, Chen SH, Liao ZK, Huang KW, Tornng PL, Hwang LH (2012) Calreticulin promotes tumor lymphocyte infiltration and enhances the antitumor effects of immunotherapy by up-regulating the endothelial expression of adhesion molecules. *Int J Cancer* 130(12):2892-2902.
45. Gajewski TF, Louahed J, Brichard VG (2010) Gene signature in melanoma associated with clinical activity: a potential clue to unlock cancer immunotherapy. *Cancer J* 16:399-403.

Figures

Fig. 1 C57BL/6 and C57BL/10 mMSC present similar molecular signaling after infection with ICOVIR-5. **a** Activation of NF- κ B after ICOVIR-5 infection was evaluated by using a luciferase reporter system. Bars represent the mCelyvir/mMSC expression ratio of NF- κ B in C57BL/6 and C57BL/10 cells. **b** Jun and pAkt expression were studied 3 h and 24 h after infection with ICOVIR-5 by Western Blot. **c** Bars in *upper panel* show the mean expression of Jun in C57BL/6 and C57BL/10 cells at 3 and 24 h. Bars in *lower panel* represent the mCelyvir/mMSC expression ratio of Jun at 3 and 24 h. **d** Bars in *upper panel* show the mean expression of pAkt in C57BL/6 and C57BL/10 cells at 3 and 24 h. Bars in *lower panel* represent the mCelyvir/mMSC expression ratio of pAkt at 3 and 24 h. Grey color represents C57BL/6 cells, while dark color represents C57BL/10 cells. Solid bars represent non-infected cells (mMSC), while stripped bars represent ICOVIR-5-infected cells (mCelyvir). * $p < 0.05$ (Will-Coxon test)

Fig. 2 Syngeneic C57BL/6 and C57BL/10 cells present similar cytokine profile secretion after loading with ICOVIR-5. **a** Secretion pattern of pro-inflammatory cytokines in C57BL/6 and C57BL/10 infected (mCelyvir) and non-infected cells (mMSC) at 24 h. The color code indicates arbitrary units of expression with white representing absence of secretion and black representing the highest secretion. **b** Bars show the mean secretion in arbitrary units of each secreted cytokine in C57BL/6 and C57BL/10 mMSC and mCelyvir. **c** ELISA to quantitate CXCL10 secretion levels in supernatants collected at 24 h post-infection. Grey color represents C57BL/6 cells, while dark color represents C57BL/10 cells. Solid bars represent non-infected cells (mMSC), while stripped bars represent ICOVIR-5-infected cells (mCelyvir). * $p < 0.05$ (Will-Coxon test)

Fig. 3 C57BL/6 and C57BL/10 mMSC and mCelyvir migrates toward tumor cells. **a** Homing ability of infected (mCelyvir) and non-infected (mMSC) cells toward CMT64-6 tumor cells was evaluated by *in vitro* transwell migration assay at 24 h. mMSC in the presence of DMEM alone was used as negative control. Images correspond to 40X power field. **b** Bars show the mean number of migrated cells per high power field (cells/HPF) at 24 h. **c** Bars represent the mCelyvir/mMSC migration ratio of C57BL/6 and C57BL/10 cells at 24 h. Grey color represents C57BL/6 cells, while dark color represents C57BL/10 cells. Solid bars represent non-infected cells (mMSC), while stripped bars represent ICOVIR-5-infected cells (mCelyvir)

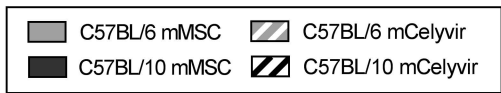
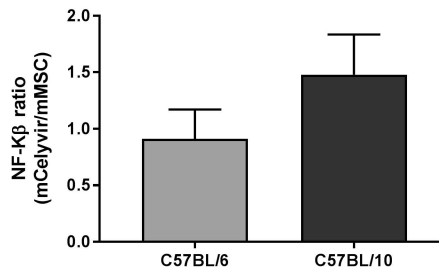
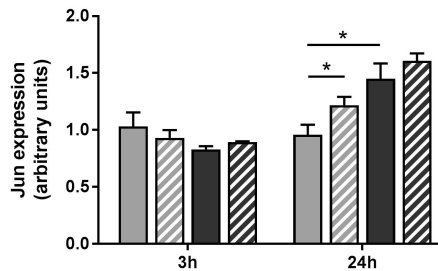
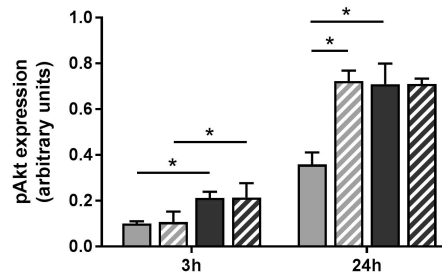
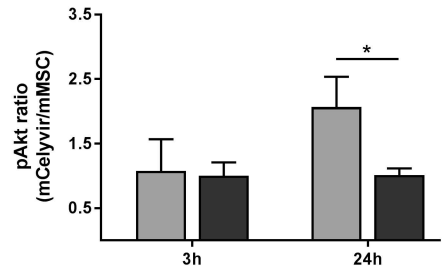
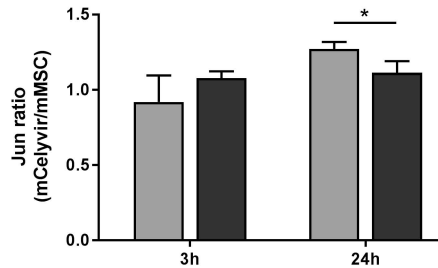
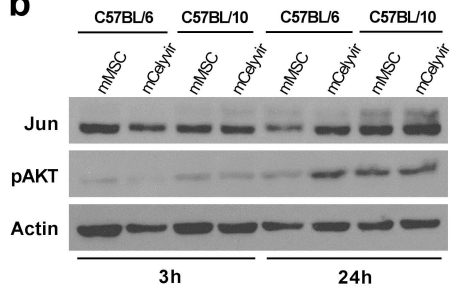
Fig. 4 Syngeneic and allogeneic mCelyvir induce a similar antitumor effect. **a** For *in vivo* experiment, CMT64-6 tumors were induced in female C57BL/6 mice by subcutaneous inoculation. PBS, syngeneic mCelyvir or allogeneic mCelyvir treatment was administered at the indicated time points. 4 weeks after the tumor inoculation, spleens were harvested and splenocytes were transferred to new CMT64-6 tumor bearing mice (1st adoptive transfer). 4 weeks after the tumor inoculation, splenocytes from transferred mice were transferred to a third group of CMT64-6 tumor bearing mice (2nd adoptive transfer). **b** Mean tumor volumes in mCelyvir treatment. **c** Individual animal measurements versus mean tumor volume of PBS group in mCelyvir experiment. **d** Mean tumor volumes in 1st adoptive transfer experiment. **e** Individual animal measurements versus mean tumor volume of PBS group in 1st adoptive transfer experiment. **f** Mean tumor volumes in 1st adoptive transfer experiment. **g** Individual animal measurements versus mean tumor volume of PBS group in 2nd adoptive transfer experiment. Red lines represent tumor volumes of mice treated with syngeneic mCelyvir and derived adoptive transfers ($n = 5$). Green lines represent tumor volume of mice treated with allogeneic mCelyvir ($n = 6$) and derived adoptive transfers ($n = 5$). Dark blue lines represent the mean tumor volume of the group treated with PBS ($n = 7$) and derived adoptive transfers ($n = 5$)

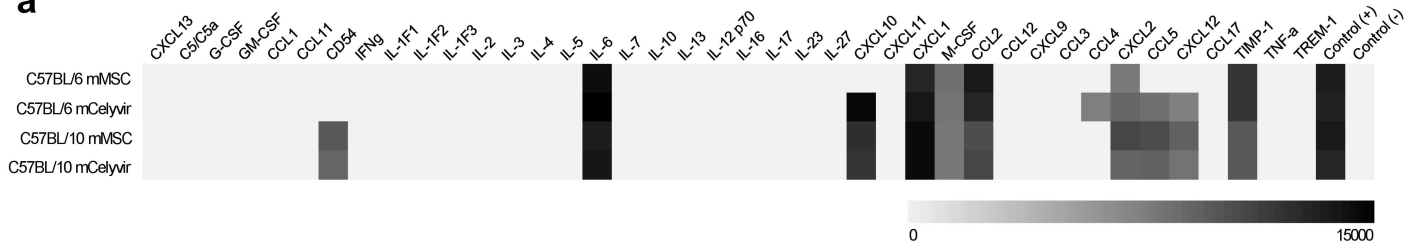
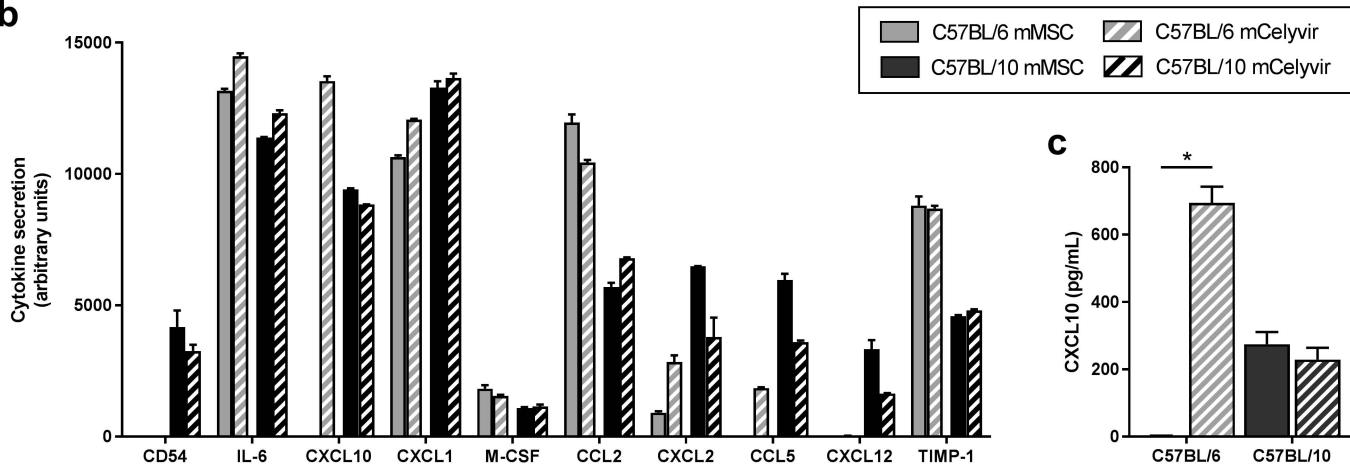
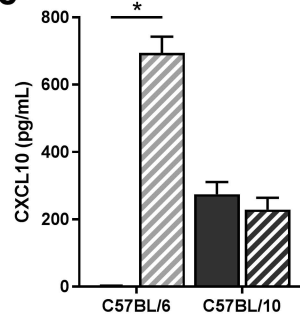
Fig. 5 mCelyvir treatment increases intratumoral N1/N2 neutrophils ratio. Percentages of tumor infiltration of CD45+ cells, CD3+ cells, CD4+/CD8+ ratio, macrophages, M1/M2 ratio, Natural Killer cells (NKs), neutrophils, and N1/N2 ratio were evaluated in groups treated with mCelyvir (**a**), 1st adoptive transfer (**b**), and 2nd adoptive transfer of splenocytes (**c**) by flow cytometry. Tumor volumes of mCelyvir-treated mice negatively correlate with N1/N2 ratios (**d**) and positively correlate with percentage of N2 (**e**). White bars represent control group ($n = 7$) and derived adoptive transfers ($n = 5$). Grey bars represent syngeneic mCelyvir-treated group ($n = 6$) and derived adoptive transfers ($n = 5$). Black bars represent allogeneic mCelyvir-treated group ($n = 6$) and derived adoptive transfers ($n = 5$). * $p < 0.05$ (Mann-Whitney *U* test)

Fig. 6 mCelyvir treatment increases leukocyte infiltration in the core of the tumor. CD45+ cells are located in the periphery of PBS-treated tumors (**a**). Tumors treated with syngeneic (**b**) or allogeneic (**c**) mCelyvir treatment show uniform distribution of CD45+ cells. Quantification of the mean fluorescence intensity (MFI) of CD45+ in the periphery and core of the tumor confirms this different pattern of tumor infiltration (**d**). Both

syngeneic (grey bars) and allogeneic mCelyvir-treated tumors (black bars) show a significant higher CD45+ core/periphery ratio compared to the control group (white bars) (e). Images correspond to representative samples. * $p < 0.05$, ** $p < 0.01$ (Mann-Whitney U test)

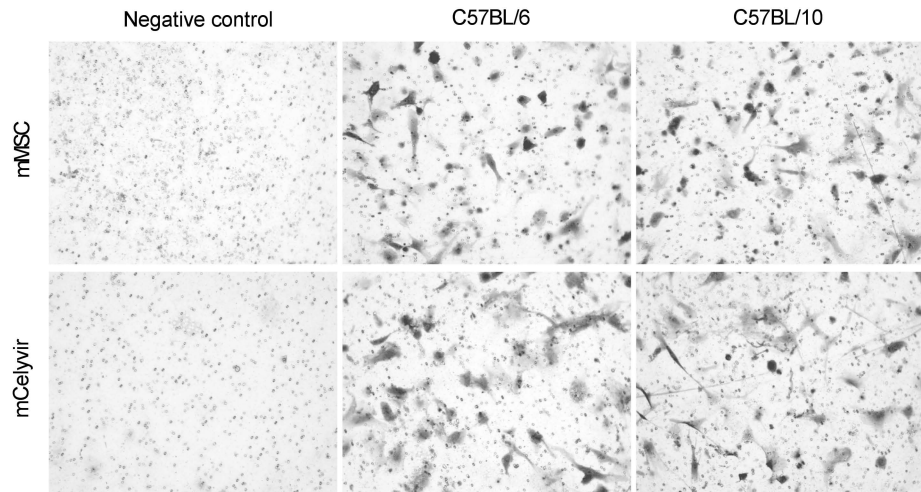
Supplementary Fig. 1 Allogeneic mCelyvir treatment reduces N2 phenotype.???? Percentages of tumor infiltration of CD4+ cells, CD8+ cells, M1, M2, N1, N2, granulocytes and dendritic cells were evaluated in mCelyvir (a), 1st adoptive transfer (b), and 2nd adoptive transfer (c) experiments by flow cytometry. White bars represent control group ($n = 7$) and derived adoptive transfers ($n = 5$). Grey bars represent syngeneic mCelyvir-treated group ($n = 6$) and derived adoptive transfers ($n = 5$). Black bars represent allogeneic mCelyvir-treated group ($n = 6$) and derived adoptive transfers ($n = 5$). * $p < 0.05$ (Mann-Whitney U test)

**a****c****d****b**

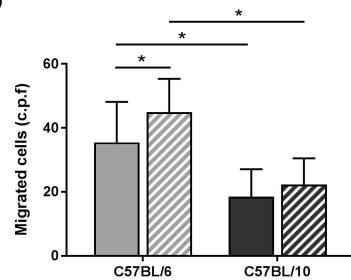
a**b****c**



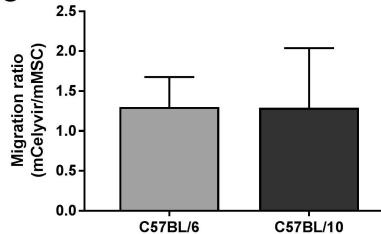
a

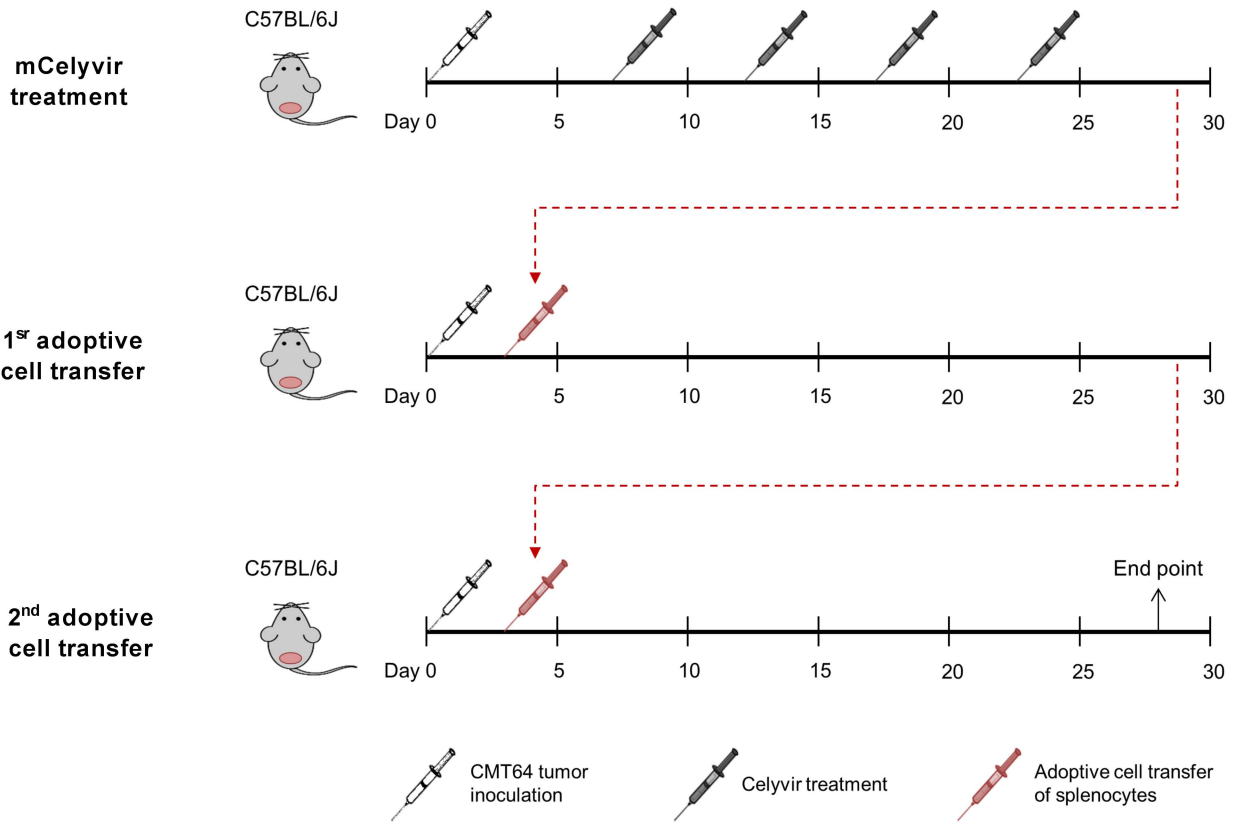
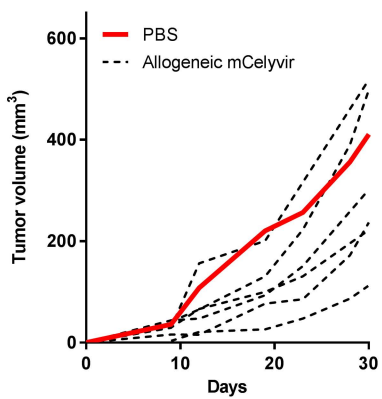
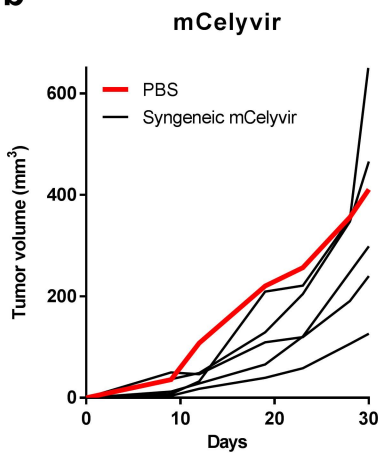
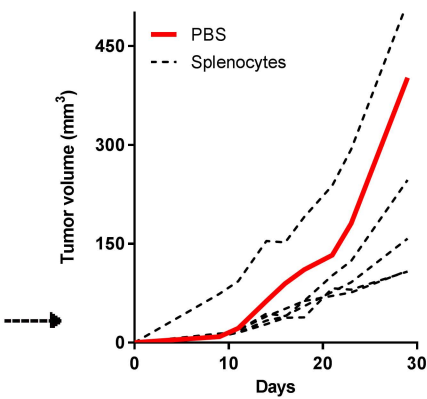
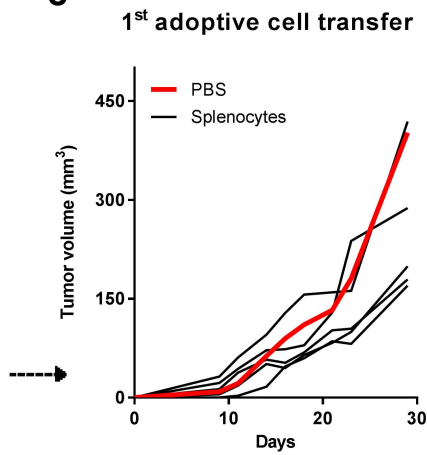
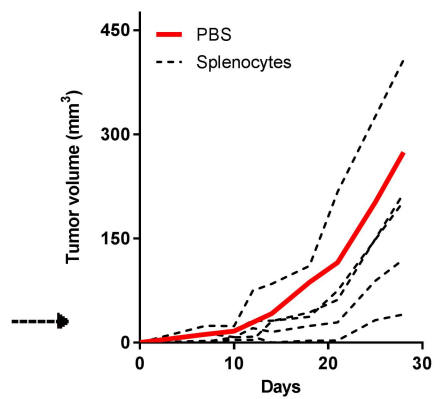
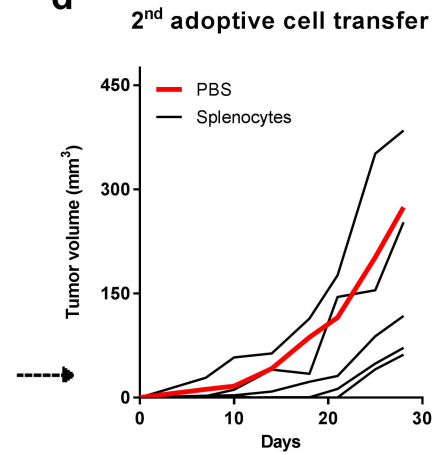


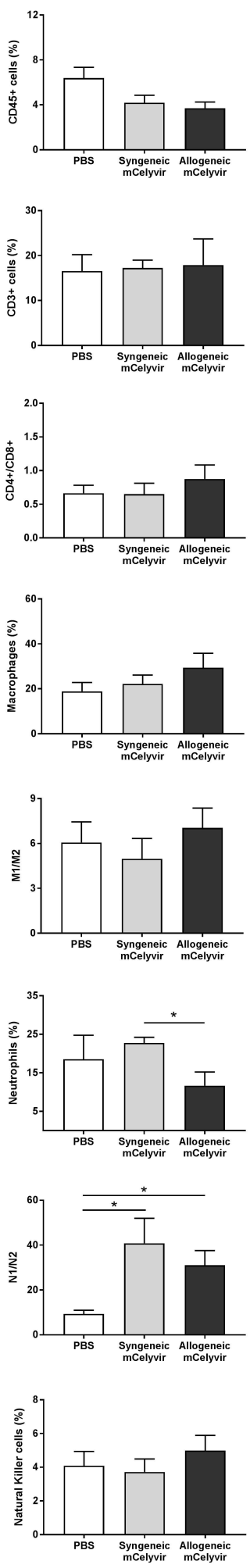
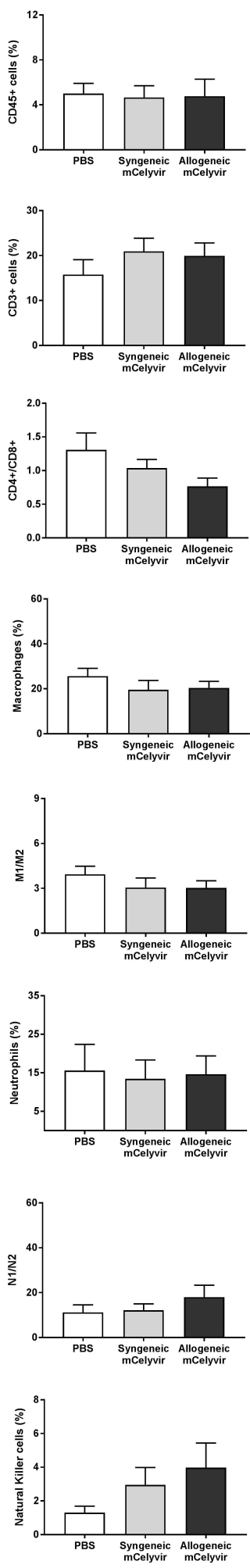
b



c



a**b****c****d**

a**mCelyvir****b****1st adoptive cell transfer****c****2nd adoptive cell transfer**